

Available online at www.sciencedirect.com

SCIENCE @ DIRECT®

Applied Surface Science 238 (2004) 410–414

applied
surface sciencewww.elsevier.com/locate/apsusc

Mesoscopic modelling of the interaction of infrared lasers with composite materials: an application to human dental enamel

A. Vila Verde^a, Marta M.D. Ramos^{a,*}, Marshall Stoneham^b, R. Mendes Ribeiro^a^a*Departamento de Física, Universidade do Minho, Campus de Gualtar, 4710-057 Braga, Portugal*^b*Department of Physics and Astronomy, University College London, Gower Street, London WC1E 6BT, UK*

Available online 8 July 2004

Abstract

The mesostructure and composition of composite materials determine their mechanical, optical and thermal properties and, consequently, their response to incident radiation. We have developed general finite element models of porous composite materials under infrared radiation to examine the influence of pore size on one of the determining parameters of the stress distribution in the material: the temperature distribution. We apply them to the specific case of human dental enamel, a material which has nanometer scale pores containing water/organic, and predict the maximum temperature reached after a single 0.35 μ s laser pulse of sub-ablative fluence by two lasers: Er:YAG (2.9 μ m) and CO₂ (10.6 μ m). For the Er:YAG laser, the results imply a strong dependence of the maximum temperature reached at the pore on the area-to-volume ratio of the pore, whereas there is little such dependence for CO₂ lasers. Thus, CO₂ lasers may produce more reproducible results than Er:YAG lasers when it comes to enamel ablation, which may be of significant interest during clinical practice.

More generally, when ablating composite materials by infrared lasers researchers should account for the material's microstructure and composition when designing experiments or interpreting results, since a more simplistic continuum approach may not be sufficient to explain differences observed during ablation of materials with similar optical properties or of the same material but using different wavelengths.

© 2004 Elsevier B.V. All rights reserved.

PACS: 42.62.-b; 42.62.Be; 44.30.+v; 02.70.Dh; 7.05.Tp

Keywords: Dental enamel; Laser ablation; Finite element modelling; Mesoscopic modelling; Er:YAG laser; CO₂ laser

1. Introduction

The mesoscopic structure and composition of a material can play a significant role in the mechanisms of laser ablation, since it determines the mechanical, thermal and optical properties of materials [1,2]. Yet, relatively few theoretical or computational models

account for this explicitly. The development of better ablation models should allow more realistic predictions of the influence of different laser parameters on ablation which will play a key role in optimizing ablation. We have developed general models to study the thermal and mechanical response of porous composite materials under infrared radiation. Here, we describe an application of these models to human dental enamel.

Currently, the ablation of dental enamel in the context of caries treatment uses Er:YAG ($\lambda = 2.9 \mu$ m)

* Corresponding author. Tel.: +351 253 604 330;

fax: +351 253 678 981.

E-mail address: marta@fisica.uminho.pt (M.M.D. Ramos).

and CO₂ ($\lambda = 10.6 \mu\text{m}$) lasers among others, but is subject to problems such as relatively low ablation rates or, when higher ablation rates are wanted, the possibility of cracking and unwanted thermal effects. If laser treatments are to become common practice, the procedures must be optimized to yield higher ablation rates while minimizing unwanted side-effects and, in the framework of minimally invasive dentistry, also ensure that precise, narrow tunnels can be drilled in teeth.

The energy of these lasers is absorbed and transformed into heat; the temperature rise is directly related to the thermal stress experienced by the material, so accurate simulation of the evolution of the material's temperature distribution is critical if we are to accurately model ablation [3]. The absorption coefficients of bulk enamel ($\lambda = 2.9$ and $10.6 \mu\text{m}$), and of the individual components of enamel (hydroxyapatite (HA) and water) at $\lambda = 10.6 \mu\text{m}$ are approximately 800 cm^{-1} [4,5]. However, the absorption coefficients of HA and water at $\lambda = 2.9 \mu\text{m}$ are far from 800 cm^{-1} . This may cause the temperature distribution at the end of an Er:YAG laser pulse to be different from the temperature distribution generated by a CO₂ laser and to depend on the mesostructure, which will undoubtedly lead to differences in stress distribution and, consequently, on ablation. The results presented consist of a finite element model of enamel, designed to study the influence of this

material's nanometer scale structure on the temperature distribution at the end of one laser pulse of sub-ablative fluence, with duration $0.35 \mu\text{s}$, by Er:YAG and CO₂ lasers.

1.1. Model description

Human dental enamel is composed mainly of HA. It is known that enamel is porous to an extent, and that the pores contain mainly water, but also a small amount of organic material; the exact proportion of water/organic, the pore size and area distributions, and pore connectivity are not known [6].

Based on this information the authors developed six finite element models for enamel (using AlgorTM Version 13.14-WIN 15-FEB-2002), each representing a piece of HA surrounding a single cubic water-pore, and used them to obtain temperature maps caused by the absorption of a sub-ablative laser pulse. The six models differ only on the size of the pore. The length of pore edges, l , varies between 30 and 130 nm (see Fig. 1).

With each model we performed transient heat transfer simulations of a single $0.35 \mu\text{s}$ laser pulse for laser radiation of $\lambda = 2.9$ and $10.6 \mu\text{m}$, using 28 timesteps of $0.0125 \mu\text{s}$ duration. We used 26,195 8-node brick elements with second order Gaussian quadrature formulation. The mesh was made significantly denser at the pore than in the zones surrounding it.

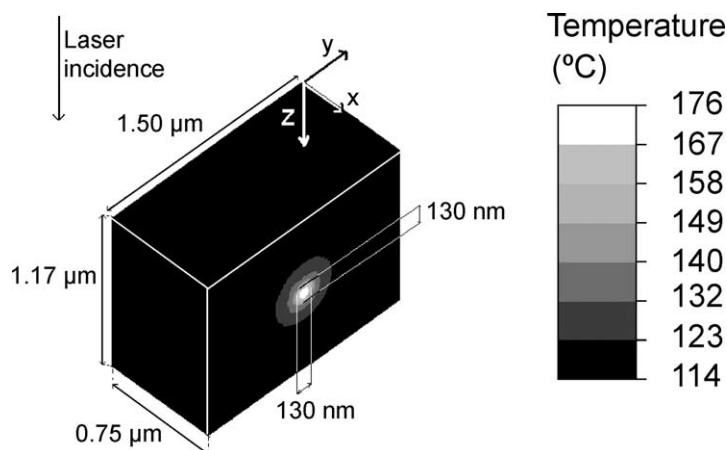


Fig. 1. Temperature map of a piece of HA surrounding a water/organic pore at the end of an Er:YAG laser pulse with the duration of $0.35 \mu\text{s}$. The dimensions of the central water/organic pore are $130 \text{ nm} \times 130 \text{ nm} \times 130 \text{ nm}$. Only half of the structure is shown.

Table 1
Material properties

	Water/organic	Mineral
Absorption coefficient at 10.6 μm (cm^{-1})	825	825
Absorption coefficient at 2.9 μm (cm^{-1})	12250 [9]	300
Thermal conductivity ($\text{J}/(\text{s m } ^\circ\text{C})$)	0.6 [5]	1.3 [11]
Specific heat ($\text{J}/(\text{kg } ^\circ\text{C})$)	4.2×10^3 [5]	8.8×10^2 [11]
Mass density (kg/m^3)	1×10^3	3×10^3 [12]

The initial temperature of the simulated structure was 37 $^\circ\text{C}$. All the material properties, which can be seen in Table 1, were considered independent of temperature. The properties of the water/organic were estimated as those of pure liquid water, since the amount of organic material is very small. The water will not undergo any phase transitions, even at the maximum temperature reached by the simulations, i.e., 175 $^\circ\text{C}$ [7]. The thermal conductivity of water (TC_{water}) varies significantly between room temperature and 175 $^\circ\text{C}$ [8], but this will have no influence on the results, because the parameter governing the maximum heat diffusion from the pore is the thermal conductivity of HA (TC_{HA}), not TC_{water} . Since we could not find experimental data in the literature on the temperature dependence of the specific heat and the thermal conductivity of HA, both were assumed constant.

The absorption coefficients of HA (α_{HA}) and water/organic (α_{water}) at 10.6 μm are considered to be the same and were given the value found in [9] for human dental enamel. Work by Shori et al. [10] indicates that α_{water} at 10.6 μm can be considered constant up to the maximum energy density (energy/volume) reached by water in these simulations. To the best of our knowledge, there is no information available in the literature regarding HA, so we adopt the same approximation for HA.

Since the authors could not find in the literature the absorption coefficient of HA at 2.9 μm , this value was estimated assuming that enamel has 4 vol.% of organic/water material and using the absorption coefficient of enamel (800 cm^{-1} [4]) and water (12,250 cm^{-1} [5]) at this wavelength.

We did not consider the effects of light scattering and assumed that all the incident laser radiation was

Table 2
Laser parameters

	Type of laser	
	CO ₂ (10.6 μm)	Er:YAG (2.94 μm)
Pulse duration (μs)	0.35	0.35
Maximum absorbed intensity, I_0 ($\text{J m}^{-2} \text{s}^{-1}$)	1.2×10^{10}	2×10^{10}
Number of pulses	1	1
Beam radius (mm)	0.2	0.2

absorbed and transformed into internal kinetic energy in a much shorter timescale than the one being simulated. The intensity at every point is given by Beer's law:

$$I(z) = I_0 \exp(-\alpha z) \quad (1)$$

where z is the depth inside the tissue, I_0 the intensity of radiation at the surface of the target and α the absorption coefficient of the tissue; it does not vary with time. The laser parameters are given in Table 2. The fluences used in the simulation (0.7 J/cm^2 for Er:YAG, 0.42 J/cm^2 for CO₂) are much below the ablation threshold of enamel, which ensures that our assumption that the geometry of the simulated structure does not change during the laser pulse is valid.

The local heat deposition, S , per unit volume and time over a slice of material with thickness ∂z is given by

$$S(z) = -\frac{\partial I(z)}{\partial z} = \alpha I(z) \quad (2)$$

The absorption of radiation by the tissue was simulated by generating heat in certain elements. The heat generating value was calculated according to Eq. (2) by taking the z coordinate of one of the element's nodes [3].

2. Results and discussion

The temperature map for the structure with a water/organic pore of $\ell = 130$ nm, under Er:YAG radiation, can be seen in Fig. 1. The pore reaches a much higher temperature than the mineral, which is predictable given the difference in the absorption coefficients of

Table 3
Maximum temperature rise at the pores for all the models

Pore dimensions (nm)	Maximum temperature rise (°C)	
	Er:YAG	CO ₂
30 × 30 × 30	81	123
50 × 50 × 50	87	123
70 × 70 × 70	97	123
90 × 90 × 90	110	123
110 × 110 × 110	125	123
130 × 130 × 130	139	123

both materials. It is clear from the image that the structure is big enough to minimize the influence of boundary effects on the temperature reached by the pore. The temperature maps for pores under CO₂ laser radiation (not displayed) show no appreciable difference between the temperature reached by the pore and mineral.

The maximum temperature rise at the pores for all the models can be seen in Table 3. For the Er:YAG laser, the temperature rise in the smallest pore (81 °C) is 60% of the temperature rise in the biggest pore (139 °C). The actual values should not be considered entirely accurate, mainly because of the uncertainty associated with the absorption coefficients of the materials, particularly the water/organic for which we used the absorption coefficient of water. We also believe that the value of α_{water} at $\lambda = 2.9 \mu\text{m}$ and TC_{HA} will most likely vary during one laser pulse. Based on the maximum energy density reached in the water (0.6 kJ/cm³), we estimate that α_{water} at this wavelength will decrease from 12250 cm⁻¹ to perhaps 10000 cm⁻¹ during the laser pulse [10]. On the other hand, TC_{HA} is estimated to vary according to 1/temperature. The combined effect of these sources of uncertainty is certainly influencing, to a small extent, the maximum temperatures reached with Er:YAG laser. Nevertheless, our results indicate that the maximum temperature reached at the pores is clearly a function of the pore volume for Er:YAG lasers, and essentially independent of pore volume for CO₂ lasers.

Since the temperature rise is directly related to the intensity of the thermal stress generated, and, ultimately, to the extent of cracking and/or ablation of material, the pore size distribution in enamel may play an important role on the ablation of this material by

Er:YAG radiation, but a less important one for ablation by CO₂ lasers.

3. Conclusions

Given the variability of the composition and mesostructure of enamel, in particular in pore size, and knowing that the thermal stress generated by laser radiation is directly related to the temperature reached, our simulations suggest that the results of ablating enamel using Er:YAG lasers may be harder to predict and reproduce from sample to sample than using CO₂ lasers. Researchers conducting experiments with these lasers, and even other IR wavelengths, may consider appropriate to select their samples attending to factors that could cause marked differences in water content, such as age or region in the tooth (see also ref. [11]). Researchers conducting in vitro experiments should also pay attention to possible differences that could arise from using hydrated or dehydrated teeth, and also teeth that were dehydrated and subsequently rehydrated.

More generally, these results suggest that one of the parameters governing ablation—the temperature—may be, for certain combinations of lasers and material properties, strongly dependent of the material's pore size and area distribution. These results suggest that in order to accurately interpret information resulting from ablation of composite materials, the material's mesostructure and composition should be considered. Researchers ablating composite materials may want to consider these material characteristics when selecting samples or analysing results.

Acknowledgements

This work was approved by the Portuguese Foundation for Science and Technology, FCT, and POCTI, and supported by the European Community Fund FEDER under project no. POCTI/ESP/37944/2001. One of us (AVV) is also indebted to FCT for financial support under Ph.D. grant no. SFRH/BD/4725/2001 and thank Mr. Richard Kramer Campen for helpful discussions during the course of this work.

References

- [1] M. Stoneham, M.M.D. Ramos, R.M. Ribeiro, *Appl. Phys. A* 69 (1999) s81.
- [2] A.M. Stoneham, J.H. Harding, *Nat. Mater.* 2 (2003) 77.
- [3] H. Niemz, Markolf, *Laser–Tissue Interactions—Fundamentals and Applications*, 1, Springer-Verlag, Berlin, 1996.
- [4] D. Fried, M.J. Zuerlein, J. Featherstone, W. Seka, C. Duhn, S.M. McCormack, *Appl. Surf. Sci.* 127–129 (1998) 852.
- [5] G.M. Hale, M.R. Querry, *Appl. Opt.* (1973) 555.
- [6] G.H. Dibdin, D.F.G. Poole, *Arch. Oral Biol.* 27 (1982) 235.
- [7] S.A. Wiesche, C. Rembe, E.P. Hofer, *Heat Mass Transfer* 35 (1999) 143.
- [8] J.R. Cooper, E.J. Le Fevre, *Thermophysical Properties of Water Substance—Student’s Tables in SI Units*, Arnold, London, 1975.
- [9] M.J. Zuerlein, D. Fried, J.D.B. Featherstone, W. Seka, *IEEE J. Selected Top. Quant. Electron.* 5 (1999) 1083.
- [10] R.K. Shori, A.A. Walston, O.M. Stafsudd, D. Fried, J.T. Walsh, *IEEE J. Selected Top. Quant. Electron.* 7 (2001) 959.
- [11] A. Vila Verde, M.M.D. Ramos, R.M. Ribeiro, A.M. Stoneham, *Thin Solid Films*, in press.